Dynamics of Cytoskeletal Proteins during Fcγ Receptor-mediated Phagocytosis in Macrophages□V

Maria Diakonova,* Gary Bokoch,† and Joel A. Swanson*‡

*Department of Microbiology and Immunology, University of Michigan Medical School, Ann Arbor, Michigan 48109-0620; and †Departments of Cell Biology and Immunology, Scripps Research Institute, La Jolla, California 92037

Particle ingestion by phagocytosis results from sequential rearrangements of the actin cytoskeleton and overlying membrane. To assemble a chronology of molecular events during phagosome formation and to examine the contributions of phosphoinositide 3-kinase (PI 3-kinase) to these dynamics, a method was developed for synchronizing Fcγ receptor-mediated phagocytosis by murine macrophages. Erythrocytes opsonized with complement component C3bi were bound to macrophages at 37°C, a condition that does not favor particle phagocytosis. Addition of soluble anti-erythrocyte IgG resulted in rapid opsonization of the bound erythrocytes, followed by their immediate internalization via phagocytosis. Cellular content of F-actin, as measured by binding of rhodamine-phalloidin, increased transiently during phagocytosis, and this increase was not diminished by inhibitors of PI 3-kinase. Immunofluorescence localization of myosins in macrophages fixed at various times during phagocytosis indicated that myosins II and IXb were concentrated in early phagosomes, myosin IC increased later, and myosin V appeared after phagosome closure. Other cytoskeletal proteins showed similar variations in the timing of their appearance in phagosomes. The PI 3-kinase inhibitor wortmannin did not change the dynamics of PI 3-kinase or ezrin localization but prevented the loss of PAK1 from phagosomes. These results suggest that PI 3-kinase deactivates PAK1, and that this may be needed for phagosome closure.

INTRODUCTION

Phagocytosis occurs by the extension of plasma membrane around an extracellular particle, followed by internalization of the particle into a membrane-bounded intracellular vesicle, the phagosome. In macrophages, different cell surface receptors stimulate different kinds of phagocytic response (Aderem and Underhill, 1999). Macrophage Fcγ receptors mediate phagocytosis of IgG-coated particles. The complement receptor CR3 binds particles opsonized with C3bi, but requires additional activation with phorbol-12-myristate-13-acetate, fibronectin, or other signals to mediate phagocytosis (Wright and Griffin, 1985).

Ligation of Fc receptors initiates an intracellular signaling cascade that impinges ultimately on the actin cytoskeleton (May and Machesky, 2001). Fcγ receptor-mediated phagocytosis can be considered a morphogenetic process, in which the actin cytoskeleton is reorganized into a cup-shaped, cell surface protrusion that constricts at its outer margin to form an enclosure (Swanson and Baer, 1995). Consistent with such a mechanism, this lab and others have experimentally distinguished two component activities of phagocytosis: pseudopod extension and phagosome closure (Araki et al., 1996; Crowley et al., 1997; Lowry et al., 1998). Pseudopod extension appears to be mediated by localized, oriented, actin polymerization beneath the plasma membrane. The mechanism of phagosome closure is not known, but apparently entails contractile activities (Swanson et al., 1999), as well as membrane insertion and vesicular trafficking (Cox et al., 1999; Bajno et al., 2000). Successful ingestion would require that the actin reorganization that extends the cell surface be coordinated temporally and spatially with the activities that close the distal margin of the phagosome. Therefore, it is appropriate to ask what molecules associate with the actin cytoskeleton during phagocytosis and when are they used in the formation of the phagosome?

Phagosome closure requires the activity of phosphoinositide 3-kinase (PI 3-kinase). Inhibitors of PI 3-kinase allow pseudopod extension, but prevent additional activities necessary for complete ingestion (Araki et al., 1996; Cox et al., 1999; Swanson et al., 1999). PI 3-kinase activity has been shown to be required for activation of Rho-family GTPases,

including Rac1 and Rho, which in turn activate downstream kinases that regulate cytoskeletal function (Cantrell, 2001). These include p21-activated kinase-1 (PAK1; Manser *et al.*, 1994) and Rho-kinase (Kimura *et al.*, 1996). Proteins regulated by these kinases include myosin light chain kinase (Sanders *et al.*, 1999) and LIM-kinase (Edwards *et al.*, 1999). Ultimately, these signaling cascades modulate actin polymerization dynamics or actomyosin-related contractile activities. The fact that PI 3-kinase inhibitors permit some activities but not others in Fcγ receptor-mediated phagocytosis indicates that the signals bifurcate early after Fcγ receptor ligation. Therefore, one may expect different cytoskeletal responses to Fcγ receptor ligation in the presence and absence of PI 3-kinase inhibitors.

The contractile activity of phagosome closure probably uses one or more classes of myosin molecule (Swanson *et al.*, 1999). Myosins localize to phagosomes (Stendahl *et al.*, 1980; Allen and Aderem, 1995), and evidently participate in the process (Ostap and Pollard, 1996), but their specific contributions to pseudopod extension or phagosome closure remain undefined. We previously localized several additional myosins in macrophage phagosomes (Swanson *et al.*, 1999). In those studies, however, no myosin labeled all phagosomes; indicating either that phagocytosis can sometimes occur without some of the myosins or that each myosin associates with phagosomes transiently.

Transient associations of proteins with phagosomes can be inferred from temporal studies. For immunofluorescence and biochemical analysis of populations of macrophages, this requires that the process be synchronized such that at each time point all cells are at the same stage in the process. Synchrony has been achieved by binding IgG-opsonized erythrocytes to macrophages at 4°C then warming the cells to initiate phagocytosis (Greenberg *et al.*, 1991; Defacque *et al.*, 2000). Such methods have obtained variable rates for Fc receptor-mediated phagocytosis. Video microscopic studies indicate that phagocytosis occurs rapidly (Swanson *et al.*, 1999). Thus, any method for synchronizing phagocytosis should obtain comparably rapid particle ingestion.

Herein, we describe an isothermal synchronization of Fcγ receptor-mediated phagocytosis in mouse macrophages. This method indicated that all cell-bound, IgG-opsonized erythrocytes could be ingested within 3 min, and allowed us to monitor the dynamics of phagocytosis-related actin polymerization. Combined use of the synchronization method with immunofluorescence microscopy provided quantitative measures of the association of myosins IC, II, V, and IXb; PAK1; ezrin; PI 3-kinase; and F-actin with forming phagosomes, and of the effects of the PI 3-kinase inhibitor wortmannin on these dynamics.

MATERIALS AND METHODS

Cells and Reagents

Bone marrow-derived macrophages were obtained from C3H/HeJ mice as described previously (Swanson, 1989). After 6 d of culture, cells were resuspended from dishes and plated onto 12-mm, circular coverslips for overnight incubation in Dulbecco's modified essential medium containing 10% heat-inactivated fetal bovine serum and penicillin/streptomycin (DM10F). Sheep erythrocytes were from the Reproductive Sciences Program, University of Michigan, Ann Arbor, MI. Other reagents were from Sigma Chemical (St. Louis, MO), unless otherwise noted.

Binding and Internalization of C3bi/RBC in Macrophages

Sheep erythrocytes coated with C3bi (E-C3bi) were prepared according to Wright and Silverstein (1982), with some modifications. Briefly, 10^9 erythrocytes in 1 ml of E-buffer (72 mM NaCl, 0.05% gelatin, 44 mM EDTA, pH 6.0) were combined with 50 μl of anti-sheep erythrocyte IgM (Calbiochem, San Diego, CA) for 30 min at 37°C, followed by 30 min at 4°C. After washing twice with D-buffer (72 mM NaCl, 0.05% gelatin, 0.5 mM MgCl$_2$, 150 μM CaCl$_2$, 2.5% glucose), the erythrocytes were incubated with 10% C5-deficient serum for 10 min at 37°C. Cells were then washed in E-buffer, and resuspended in D-buffer. E-C3bi (0.5 ml at 10^9 cells/ml) were added in 0.5 ml of warm Ringer's buffer (RB: 155 mM NaCl, 5 mM KCl, 1 mM MgCl$_2$, 2 mM CaCl$_2$, 2 mM Na$_2$HPO$_4$, 10 mM glucose, 10 mM HEPES, pH 7.2) to each well containing macrophages on 12-mm coverslips (1.5–3.5 × 10^5 cells/well). A brief centrifugation (500 rpm, 1 min), followed by 2 min at 37°C provided optimal E-C3bi binding to the macrophages (longer incubations increased background levels of uptake, reaching 1–1.8 E-C3bi/macrophage after 10 min; our unpublished results). After several seconds of washing with warm RB, rabbit anti-E IgG (ICN Biomedicals, Aurora, OH) at 1:100 dilution in RB were added to the coverslips to stimulate phagocytosis.

For binding experiments, cells were fixed for 30 min in 4% formaldehyde in 40 mM HEPES, pH 7.3, 6.8% sucrose then the number of erythrocytes per 100 macrophages was determined. The binding index was reported as the number of erythrocytes per macrophage. To identify internalized erythrocytes, extracellular erythrocytes were lysed by a 30-s exposure to distilled water then macrophages were fixed and scored as described above.

Video Microscopy

For video microscopic study of phagocytosis, 25-mm circular coverslips with adherent macrophages were assembled into Leiden chambers (Harvard Apparatus, Cambridge, MA), with 1 ml of RB. Cells were observed by phase contrast optics in a Nikon TE300 inverted microscope with shutter-controlled illumination (Uniblitz, Rochester, NY). For asynchronous phagocytosis, IgG-opsonized erythrocytes (Knapp and Swanson, 1990) were added to buffer and allowed to land on the macrophages. For synchronous phagocytosis, E-C3bi were bound to macrophages on coverslips and recorded; after 2 min, opsonizing anti-E IgG was added to the chamber and images were recorded for another 15 min. All images were collected using a cooled, digital charge-coupled device camera (Quantix; Photometrics, Tucson, AZ) and were recorded (1 frame/10 s) and stored using MetaMorph software (Universal Imaging, West Chester, PA). Quicktime movies of the image stacks were prepared using MetaMorph and Premiere 5.0 (Adobe Systems, San Jose, CA).

Scanning Electron Micrsocopy

Macrophages on coverslips were bound with E-C3bi as described above then opsonizing anti-E IgG was added. At 10-s intervals, pairs of coverslips were fixed with 2% glutaraldehyde (Ted Pella, Redding, CA) in 0.1 M cacodylate buffer, pH 7.4, containing 6.8% sucrose, for 1 h at room temperature (Araki *et al.*, 1996). Coverslips were then postfixed with 1% osmium tetroxide (Ted Pella) in 0.1 M cacodylate buffer for 1 h at 4°C, and treated with 1% tannic acid in distilled water for 30 min, and then 1% osmium tetroxide for 30 min at 4°C. After dehydration in a graded ethanol series, they were treated with hexamethyldisilazane (Ted Pella) for 10 min and dried overnight. Specimens were coated with platinum by using an iron-coater and observed with a scanning electron microscope (DS130; Topcon, Tokyo, Japan).

Quantitative Measure of F-actin

F-actin was quantitated using a rhodamine-phalloidin binding assay originally developed by Howard and Oresajo (1985) and mod-

ified by Cano *et al.* (1991). Macrophages were plated at 3.5×10^5 cells/coverslip for phagocytosis experiments and 1.5×10^5 cells/ coverslip for macrophage colony-stimulating factor (M-CSF) treatment experiments. Before each experiment, macrophages were incubated with prewarmed RB for 30 min at 37°C. E-C3bi were incubated with macrophages as described above, and phagocytosis was initiated by adding anti-E IgG. At 15- or 30-s intervals, a coverslip was removed and fixed, for 20 min with 3.7% formalin in 1% Triton X-100, and then stained with 0.2 μM rhodamine-phalloidin for 30 min. After washing, the cells were extracted with 2 ml of methanol for 1 h in the dark. Rhodamine fluorescence (excitation 540 nm, emmission 575 nm) was measured using an SPF-500C spectrofluorometer (SLM/Aminco, Urbana, IL). To normalize for cell number, nuclei were stained with 2 μg/ml 4,6-diamidino-2-phenylindole for 10 min and, after washing, cells were scraped off of the dishes. Fluorescence was determined (excitation 358 nm, emission 461 nm) after allowing 5 min for cellular debris to settle. F-actin content per cell was calculated as the ratio of rhodamine-phalloidin to 4,6-diamidino-2-phenylindole (nuclear) fluorescence. Nonsaturable binding of the rhodamine-phalloidin, determined by incubating samples in rhodamine-phalloidin plus 100-fold excess (20 μM) of unlabeled phalloidin, contributed 13% of the signal. Effects of cytochalasin D were assayed after a 15-s incubation of E-C3bi-bound macrophages with anti-E IgG. Wortmannin (100 nM) and LY294002 (50 μM) were added to E-C3bi-bound cells 5 min before IgG addition. For treatments with M-CSF, macrophages were incubated 15 min in RB then were treated with M-CSF (3000 unit/ ml; R & D Systems, Minneapolis, MN) in the same buffer.

Immunofluorescence

Macrophages on 12-mm coverslips were incubated 30 min with RB. E-C3bi (10^7/coverslip) were bound to macrophages as described above. To initiate phagocytosis, monoclonal mouse anti-E IgG (affinity-purified IgG, MAS 013; Harlan Sera-Lab, Leicestershire, United Kingdom) was added in 1:100 dilution in RB at 37°C. At 10-s intervals, coverslips were removed and fixed with CFA (4% paraformaldehyde, 5% polyethylene glycol 400 in intracellular buffer [IB]: 30 mM HEPES, pH 7.4, 10 mM EGTA, 0.5 mM EDTA, 5 mM MgSO$_4$, 33 mM potassium acetate, and 0.02% sodium azide), 15 min at 37°C, and were permeabilized with CFB (1% Triton X-100, 4% paraformaldehyde, 5% polyethylene glycol 400 in IB) for 15 min at 37°C. Nonspecific staining was reduced by incubation 3 × 5 min in 2% goat serum in IB. Goat antimouse IgG labeled with 6-((7-amino-4-methylcoumarin-3-acetyl)amino)hexanoic acid (AMCA) or Texas Red (Molecular Probes, Eugene, OR) was added to coverslips together with rabbit polyclonal antibodies recognizing PAK1 (Dharmawardhane *et al.*, 1997), the p85 subunit of PI 3-kinase (06-195; Upstate Biotechnology, Lake Placid, NY), ezrin (Upstate Biotechnology), myosin IC (Skowron *et al.*, 1998), myosin II (Biomedical Technologies, Stoughton, MA), myosin V (Espreafico *et al.*, 1992) or myosin IXb (Wirth *et al.*, 1996). After a second wash (3 × 5 min with 2% goat serum in IB), cells were labeled with Oregon Green-labeled anti-rabbit IgG (1:10,000 dilution; Molecular Probes), with or without Texas Red-phalloidin (for experiments with AMCA-goat antimouse IgG) (1:40 dilution). Coverslips were postfixed with CFA for 15 min then mounted in glycerol with 1 mg/ml phenylenediamine for viewing. Images were collected with a laser scanning confocal microscope (Noran Instruments, Middleton, WI) with a 100× objective lens, by using settings for simultaneous imaging of Texas Red-labeled erythrocytes and Oregon Green-labeled proteins of interest. AMCA-labeled erythrocytes and associated fluorescence for quantitative studies were scored using a widefield fluorescence microscope (Axioskop; Zeiss, Thornwood, NY), with filter sets for UV, fluorescein, and Texas Red. Samples were masked and coded for blinded scoring; for each condition and time point, 200 AMCA-positive phagosomes were scored for bright Oregon Green fluorescence surrounding the particle.
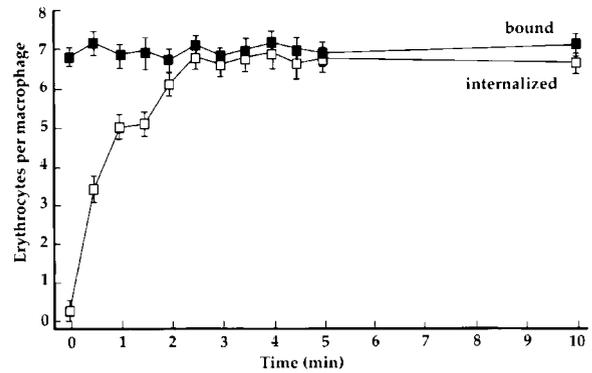
Figure 1. Binding and internalization of erythrocytes. Sheep erythrocytes were coated with C3bi, and bound to macrophages at 37°C. Rabbit anti-E IgG was then added to initiate phagocytosis (time 0). At the indicated times, macrophages either were fixed (bound, ■) or were exposed to distilled water for 30 s to lyse extracellular erythrocytes, and then fixed (internalized, □). The number of cell-associated erythrocytes per 100 macrophages was counted then plotted as erythrocytes per macrophage. Data are the mean and SEM pooled from three separate experiments.

RESULTS

Synchronous Fcγ Receptor-mediated Phagocytosis

Synchronized phagocytosis at constant temperature was obtained using mouse bone marrow-derived macrophages and sheep erythrocytes opsonized with C3bi (E-C3bi). These erythrocytes bound to macrophages at 37°C but were not phagocytosed. Addition of soluble rabbit anti-E IgG opsonized the bound erythrocytes and initiated Fcγ receptor-mediated phagocytosis.

The synchrony of the phagocytosis stimulated by addition of IgG was measured by direct counting, and was supported by video and scanning electron microscopy. At various times after addition of IgG, cells were fixed and examined by phase-contrast light microscopy to quantify cell-associated and internalized erythrocytes. The number of cell-associated erythrocytes did not change during 10 min of incubation with IgG, whereas the number of internalized erythrocytes increased rapidly during the first 2 min, saturating by 3 min after IgG addition (Figure 1).

Video microscopic data indicated that Fcγ receptor-mediated phagocytosis occurred rapidly. When E-IgG was added to macrophages to allow asynchronous phagocytosis, particles bound to cells at various times over the 30 min of observation. Erythrocyte ingestion, detectable as a change in particle contrast from phase-bright to phase-dark, began at different times after binding, but happened quickly once it started (Figure 2A; and accompanying video sequence). In contrast, macrophages with bound E-C3bi did not ingest particles until anti-E IgG was added, whereupon the cell-bound erythrocytes changed relatively synchronously, over the course of 2–4 min, from phase-bright to phase-dark (Figure 2B; and accompanying video sequence). Up to 28 min was required for complete ingestion of erythrocytes by asynchronous phagocytosis, whereas synchronized phagocytosis was essentially completed by 7 min (Figure 2).

Scanning electron microscopy showed many erythrocytes bound to surfaces of well-spreaded macrophages, but few
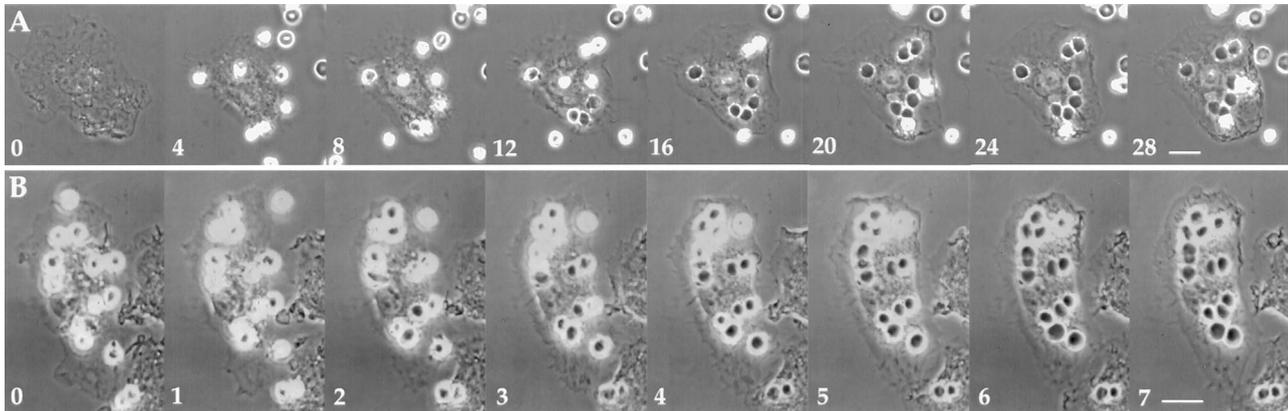
Figure 2. Video microscopy of Fcγ receptor-mediated phagocytosis. Time-lapse, phase-contrast microscopy shows asynchronous phagocytosis of E-IgG (A) and synchronous phagocytosis of E-C3bi after addition of anti-E IgG (B). Elapsed times after the left-most frame are indicated, in minutes, in the lower left corner of each frame. (A) At time 0, E-IgG was added to the wells and images were collected (1 frame/10 s). E-IgG contacted the macrophage and were subsequently ingested (transition from phase-bright to phase-dark) at different times over the next 28 min (video available as Asynch.mov). (B) At time 0, anti-E IgG was added to macrophages with prebound E-C3bi; images were collected regularly thereafter. The erythrocytes were ingested as a cohort within the next 5 min (video available as Synch.mov). Scale bar, 10 μm.

were internalized without IgG treatment (Figure 3A). Ten and 20 s after addition of IgG, however, many erythrocytes could be observed in cup-like macrophage pseudopodia (Figure 3, B and C). In cells fixed at 2 min, most erythrocytes were enclosed by pseudopodia (Figure 3D).

Dynamics of Actin Polymerization during Phagocytosis and Pinocytosis

The content of F-actin in cells was obtained by measuring the binding of rhodamine-phalloidin. E-C3bi were bound to macrophages then anti-E IgG was added to initiate phagocytosis. A rapid rise in the F-actin content followed in the first 15 s, followed by a slight decrease, with a second burst of actin assembly after 60 s (Figure 4A). By 3 min, when phagocytosis was completed, the F-actin content of macrophages had declined to its initial levels. Control experiments indicated that the actin polymerization was associated with phagocytosis. Addition of anti-E IgG to macrophages without bound E-C3bi elicited no changes in F-actin content (Figure 4A). Moreover, addition of irrelevant anti-dinitrophenyl antibodies to E-C3bi-bound macrophages did not stimulate changes in F-actin content (Figure 4A). Thus, the increase in actin polymer content correlated with the initiation of phagocytosis.

With a precise measurement of the change in F-actin, we examined the effects of several drugs that inhibit phagocytosis. Cytochalasin D added before addition of E-C3bi prevented their binding to macrophages. We therefore incubated E-C3bi with macrophages, initiated phagocytosis by addition of anti-E IgG, and added cytochalasin D 15 s later. By this protocol, the number of bound E-C3bi did not change, but the number of internalized erythrocytes remained close to background levels (our unpublished results). The increase in actin polymer content, apparent at 15 s after IgG treatment, dropped to control levels after addition of cytochalasin D (Figure 4B). The PI 3-kinase inhibitors wortmannin and LY294002 dramatically inhibited the

phagocytosis of IgG-opsonized erythrocytes. Wortmannin did not inhibit the binding of E-C3bi to macrophages, but prevented internalization after addition of anti-E IgG. The phagocytic indices of macrophages 2 min after addition of IgG were 4.14 ± 0.75 for control and 1.84 ± 0.25 for wortmannin-treated cells (binding indices were 4.59 ± 0.30 and 4.36 ± 0.84 for control and wortmannin-treated cells, respectively; n = 5). Examination of the effect of wortmannin and LY294002 on phagocytosis-related changes in actin polymer content revealed increased F-actin during the first 60 s of internalization, followed by a decline to initial levels within 1–2 min (Figure 4B). This was consistent with an earlier report showing that wortmannin did not inhibit Fcγ receptor-mediated changes in F-actin content (Cox *et al.*, 1999).

M-CSF stimulates macropinocytosis as well as ruffling in macrophages (Racoosin and Swanson, 1989), and wortmannin and LY294002 inhibit macropinocytosis but not ruffling (Araki *et al.*, 1996). We measured F-actin content in macrophages stimulated with M-CSF. Macrophages increased their actin polymer content in response to M-CSF (Figure 4C), obtaining maximal levels at 30 s. In contrast to their effects on Fcγ receptor-mediated responses, preincubation of macrophages with wortmannin or LY294002 inhibited M-CSF–induced increases in F-actin content (Figure 4C).

Redistributions of Cytoskeletal Proteins during Phagocytosis

The methods for synchronizing Fcγ receptor-mediated phagocytosis allowed us to order the sequence of myosin associations with forming phagosomes. Macrophages with bound E-C3bi were fixed at various intervals after addition of anti-E IgG, and were prepared for immunolocalization of myosins IC, II, V, or IXb, plus the anti-E IgG. Phagosomes were observed by fluorescence confocal microscopy, and corresponding images of both erythrocyte membranes and myosin localization were collected (Figure 5). Macrophages fixed 20–30 s after addition of IgG showed erythrocytes
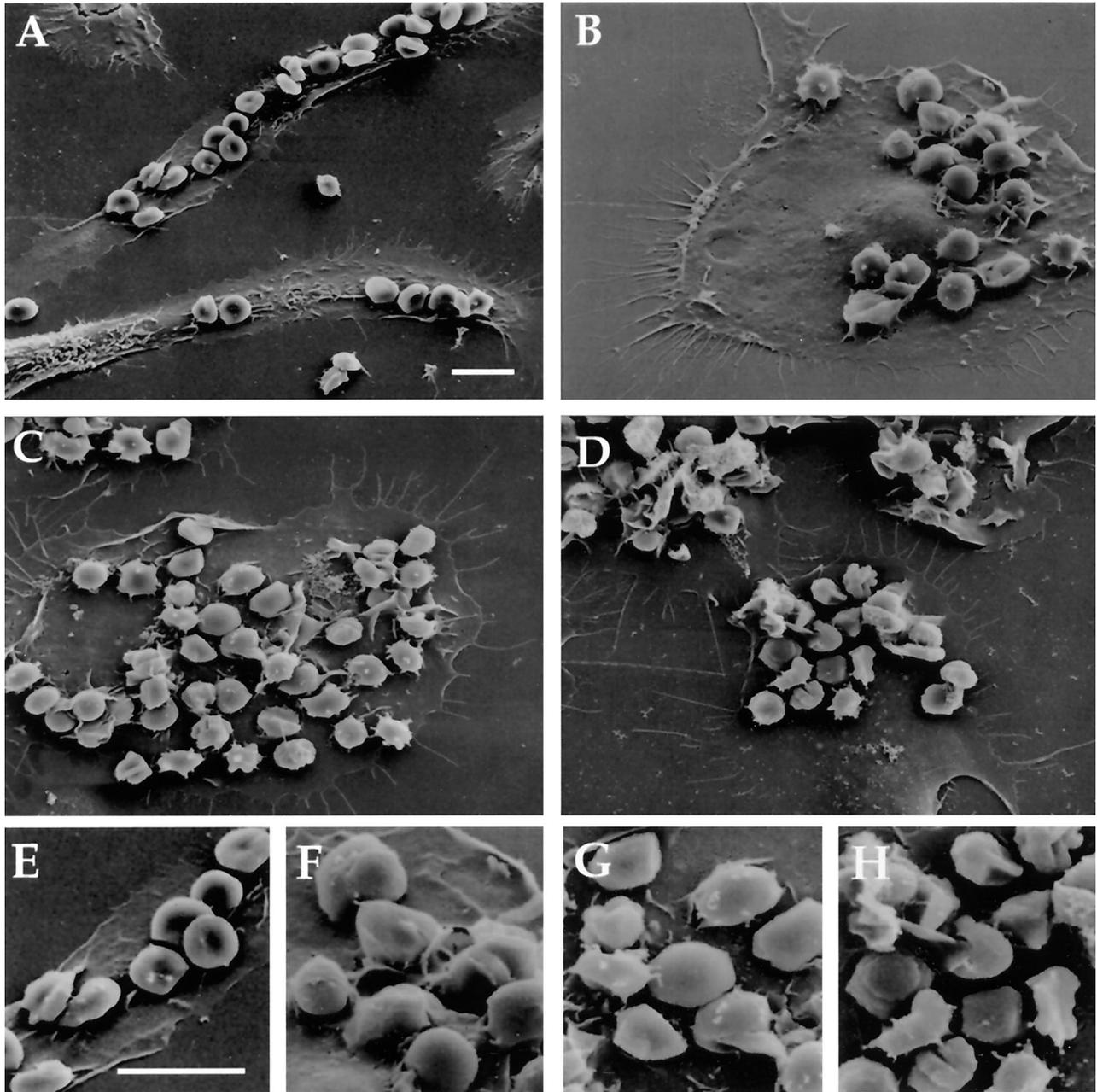
Figure 3. Scanning electron microscopy of synchronized phagocytosis. Macrophages with bound erythrocytes were fixed at various times after addition of anti-E IgG. At time 0, the erythrocytes were bound to the macrophages, but not internalized (A). Ten seconds after addition of anti-E IgG, phagocytic cups were evident around some erythrocytes (B). By 20 s, many of the erythrocytes had been engulfed (C) and by 2 min many more were contained within macrophage surface extensions (D). (E-H) Enlarged portions of A-D, respectively. Scale bar, 10 μm.

surrounded with myosins IC, II, and IXb; with few if any staining positive for myosin V (Figure 5, A-H). In contrast, cells fixed 3 min after addition of IgG showed diminished labeling for myosins IC, II, and IXb, and increased labeling with antibodies against myosin V (Figure 5, I-P).

Myosin distributions during synchronized phagocytosis were quantified. Cells were fixed at 10–20-s intervals after addition of IgG, and for every time point, 200 phagosomes in labeled cells were counted and scored for the presence of myosin (Figure 6A). Myosins II and IXb showed a peak of association with phagosomes 20 s after addition of IgG, whereas myosin IC association peaked 30 s after IgG addition. Associations increased again at later times. Myosin V association with phagosomes was initially low, and increased continuously during 3 min. Wortmannin dramatically decreased the association of myosins with phagosomes
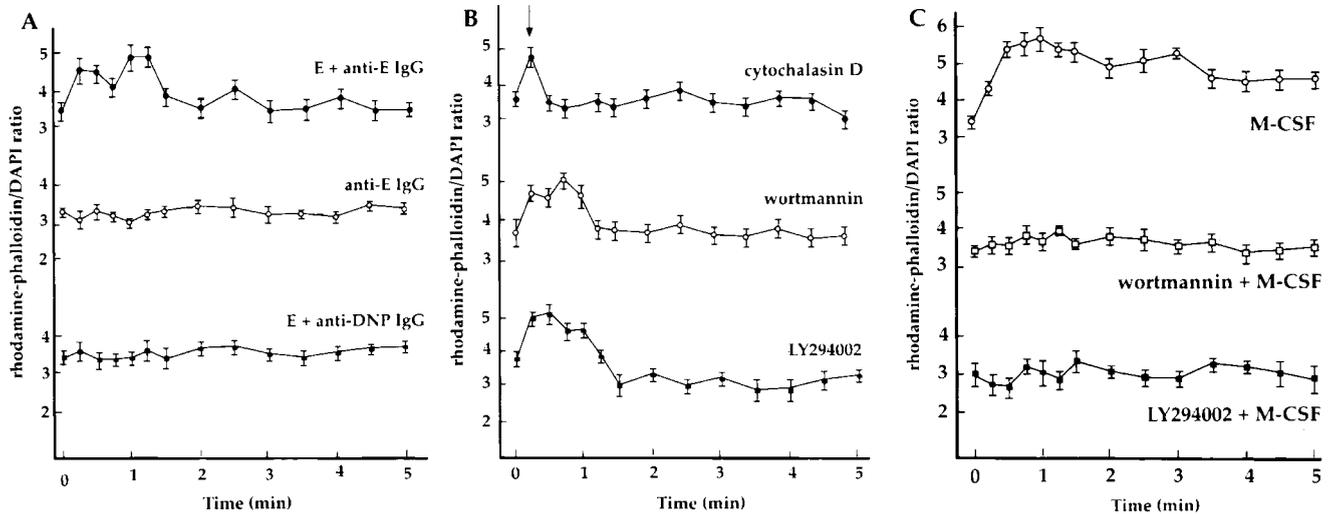
Figure 4. Dynamics of actin polymerization during synchronized phagocytosis and after stimulation with M-CSF. Rhodamine-phalloidin binding was measured in lysates of cells permeabilized at the indicated times after addition of IgG. (A) In macrophages with bound E-C3bi, a rapid rise in the F-actin content occurred during the first 15 s after addition of anti-E IgG, and again 60 s later (●). No change in actin polymer content was detected when anti-E IgG was added in the absence of bound erythrocytes (○), or after adding irrelevant anti-dinitrophenyl IgG to cell-bound E-C3bi (■). (B) Changes in F-actin associated with inhibition of Fcγ receptor-mediated phagocytosis. Cytochalasin D (5 μM) added 15 s after the addition of anti-E IgG (arrowhead) inhibited further actin polymerization (●). Wortmannin (100 nM, ○) or 50 μM LY294002 (■) did not inhibit IgG-stimulated actin polymerization. (C) Effect of M-CSF on actin polymerization. M-CSF stimulated a rapid and sustained increase actin polymer content (○). Cells pretreated with wortmannin (□) or LY294002 (■) did not increase total F-actin content in response to M-CSF.

(Figure 6B), although it had no detectable effects on the overall levels of fluorescence. The most pronounced effect of wortmannin was observed for myosins V and IXb: a slight peak of association of myosin V at 30 s was followed by slightly elevated labeling for 3 min (Figure 6B). Myosin IXb did not translocate to phagosomes in presence of wortmannin.

Synchronization and immunofluorescence were also used to analyze the associations of other proteins with phagosomes (Figure 6C). Antibodies to the p85 subunit of PI 3-kinase labeled phagosomes maximally at 30 s after addition of IgG. PAK1 associated maximally at 40 s, and ezrin labeled phagosomes gradually, peaking at 40 s and remaining high. A peak of F-actin–stained cup-like structures occurred at 20 s, corresponding to the first peak of F-actin measured in lysates (Figure 4A).

F-actin, PI 3-kinase, PAK1, and ezrin were also localized in the unclosed phagosomes of macrophages exposed to wortmannin. Curiously, all antibodies were detectable on phagosomal membranes, although the timing and extent of their associations differed. Rhodamine-phalloidin labeled fewer phagosomes than in control experiments (Figure 6D). Wortmannin did not affect the dynamics of PI 3-kinase and ezrin, but prevented the loss of PAK1 from the unclosed phagosomes (Figure 6D).

Thus, although wortmannin did not reduce Fcγ receptor-stimulated actin polymerization, it inhibited the association of myosins and the dissociation of PAK1 from phagosomes. These altered dynamics could underlie wortmannin's inhibition of phagosome closure.

DISCUSSION

Fluorescent molecular probes observed in single living macrophages have revealed much about molecular timing and localization during phagocytosis (Swanson *et al.*, 1999; Botelho *et al.*, 2000). Proper studies of this kind are difficult to analyze quantitatively, however, and many kinds of biochemical information must still be obtained from populations of cells undergoing phagocytosis synchronously. Synchrony can be achieved by prebinding particles to macrophage surfaces at low temperatures, which inhibit phagocytosis, then warming to initiate ingestion (Greenberg *et al.*, 1991; Defacque *et al.*, 2000). However, these protocols produce variable rates of phagocytosis, and may produce artifacts due to the temperature shifts.

The present method for synchronizing phagocytosis produced good temporal resolution for biochemical and immunohistochemical studies without the use of temperature shifts. E-C3bi were bound to macrophages via the receptor CR3, which does not mediate phagocytosis without additional activation (Wright and Griffin, 1985). E-C3bi tethered in this way were positioned for phagocytosis, and addition of soluble anti-E IgG coated the erythrocytes quickly and initiated a rapid phagocytic response; complete ingestion occurred within 3 min. Time-lapse video microscopy of the response indicated that the ingestion was nearly synchronous. The method allowed biochemical study of the dynamics of actin polymerization, and measurement of the timing of the arrival and departure of various cytoskeletal proteins. It also allowed an analysis of the relative effects of wortmannin on these dynamics.
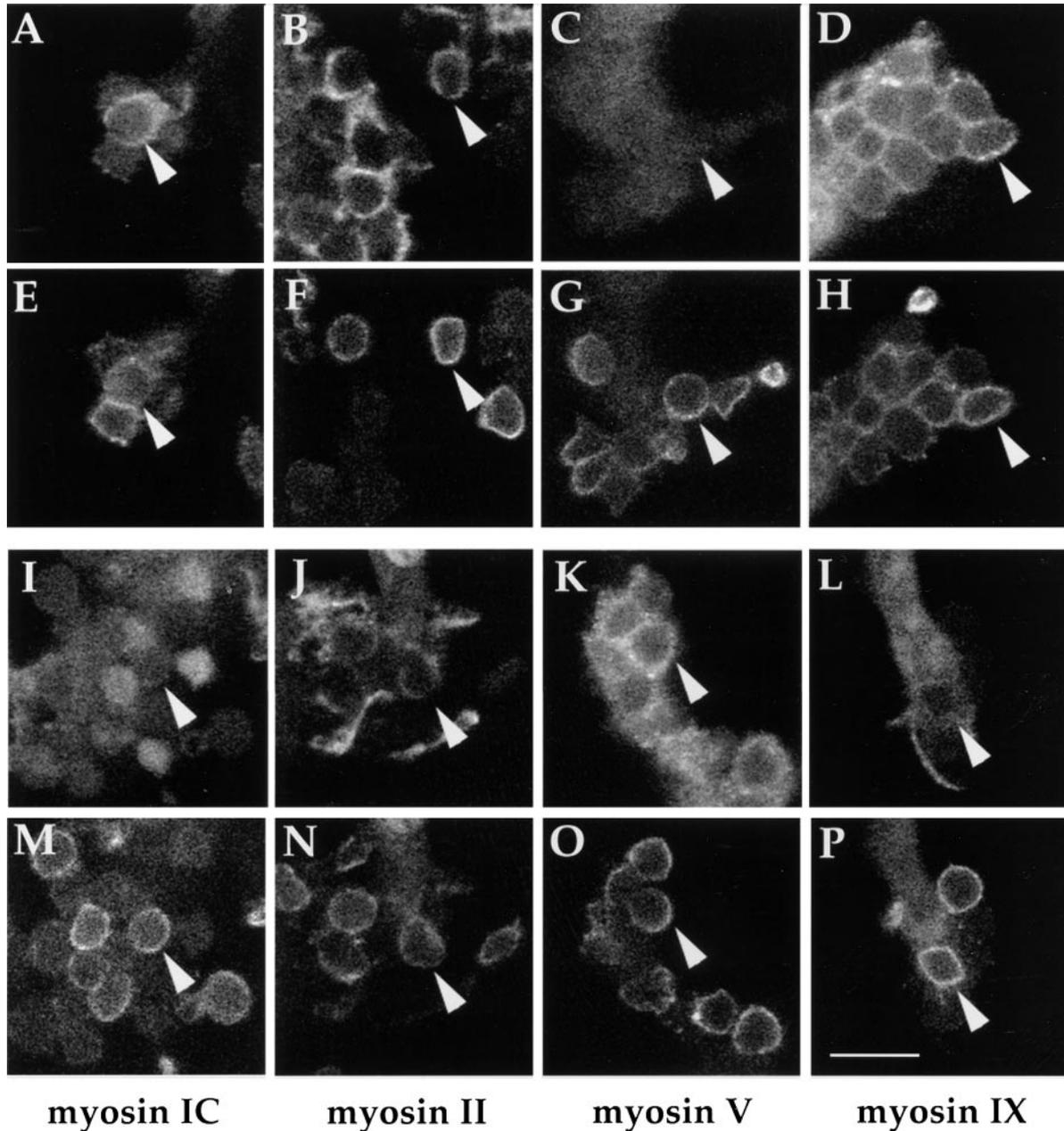
Figure 5. Immunofluorescence of myosin distributions during synchronized phagocytosis. Phagocytosis was initiated by addition of monoclonal mouse anti-E IgG to macrophages with bound C3bi. Cells were fixed at 30 s (A-H) or 3 min (I-P), and stained with anti-myosin primary antibodies (rabbit IgG) plus Oregon Green-labeled goat antirabbit IgG (A-D, I-L), and with Texas Red-labeled goat antimouse IgG, to recognize erythrocytes (E-H, M-P). Confocal optical sections were taken as through-focus series of phagosomes. Corresponding images of myosin labeling and erythrocyte-associated IgG are stacked (e.g., A with E, B with F, etc.). Myosins IC, II, and IX b associated with phagosomes more at 30 s that at 3 min. Conversely, phagosome labeling for myosin V was low early and more prominent later. Arrowheads indicate corresponding phagosomes in image pairs. Scale bar, 10 μm.

The phagocytic response began with a rapid increase in cellular F-actin. The rhodamine-phalloidin binding assay indicated peaks of F-actin at 20 and 60 s after addition of IgG. Additional increases at 2.5 and 4 min indicated a possible dampening oscillation of cellular F-actin content in response to the phagocytic stimulus. These responses required phagocytosis, because they were absent in control conditions in which phagocytosis either did not occur or was inhibited by cytochalasin D. Biphasic increases in F-actin were noted previously (Greenberg *et al.*, 1991), and a recent
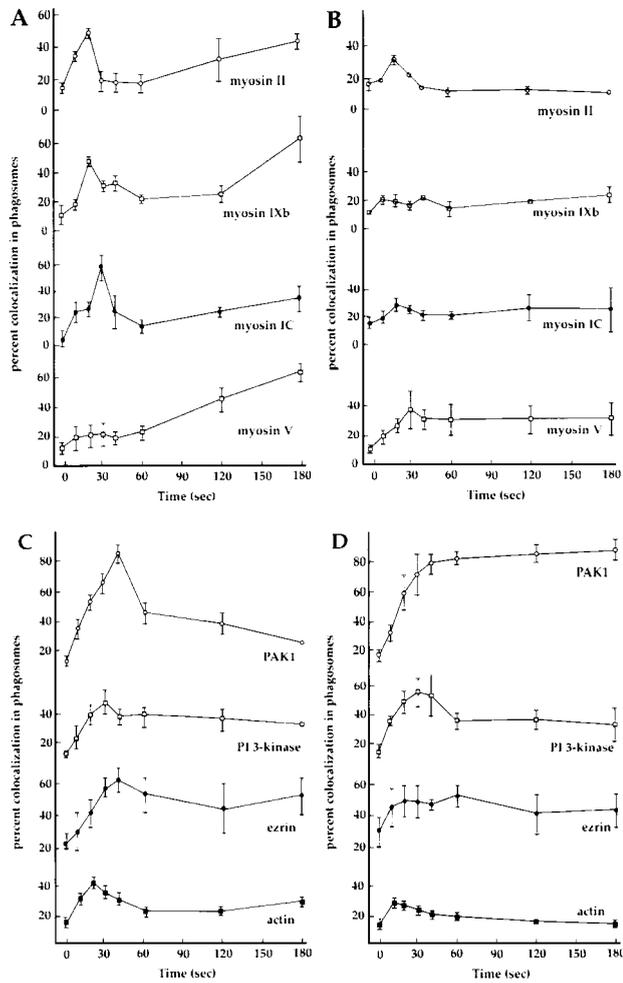
Figure 6. Association of myosins, PI 3-kinase, PAK1, ezrin, and F-actin with phagosomes. Phagocytosis was synchronized by addition of anti-E IgG to macrophages with bound E-C3bi (time 0). (A and B) At the indicated times thereafter, cells were fixed and processed for immunofluorescence localization of the anti-E IgG (AMCA-labeled), plus either myosin IC, II, V, or IXb. The fraction of phagosomes positive for each myosin was determined. Each point shows the mean and SEM for the pooled data of three experiments (200 measured particles per experiment). Myosins II and IXb both showed maximal association with phagosomes at 20 s, and myosin IC associated maximally at 30 s. Myosin V was initially not associated with phagosomes but increased its association gradually. All myosins showed some increased association with phagosomes at later time points. (B) Wortmannin inhibited association of myosins with phagosomes. Macrophages with bound E-C3bi were treated with wortmannin for 5 min and then anti-E IgG was added. Phagocytosis was inhibited, and little or no increase in myosin labeling was detected. (C and D) At the indicated times after addition of anti-E IgG to stimulate phagocytosis, macrophages were fixed and stained to localize the anti-E IgG, plus either PAK1, PI 3-kinase, ezrin (Oregon Green-labeled secondary antibodies) or F-actin (Texas Red-phalloidin). (C) Maximal labeling for PI 3-kinase occurred at 30 s, and for PAK1 and ezrin at 40 s. Actin maximally associated with phagosomes at 20 s, which corresponded to the first peak of actin-polymerization measured in lysates (Figure 4A). (D) Pretreatment with wortmannin did not substantially alter the dynamics of PI 3-kinase, ezrin, or F-actin association with phagosomes, but prevented the loss of PAK1 from phagocytic cups. Each point shows the mean and SEM for the pooled data of three experiments (200 measured particles per experiment).

study detected biphasic changes in F-actin with kinetics similar to those reported herein (Defacque *et al.*, 2000). In the present studies, the first peak of F-actin at 20 s correlated with the single peak of phagosome-associated F-actin measured by quantitative fluorescence microscopy (Figure 6C). The second peak was not observed in the microscopic assay, which indicates that it was initiated by phagocytosis but was not associated with the phagosome. Time-lapse video microscopy of phagocytosis sometimes indicates a burst of ruffling or macropinocytosis near a forming phagosome (our unpublished results), and the second peak of F-actin could be related to these delocalized cytoskeletal responses.

The PI 3-kinase inhibitors wortmannin and LY294002 inhibit phagosome closure but not pseudopod extension, and macrophages in wortmannin form phagocytic cups that do not close (Araki *et al.*, 1996). Pseudopod extension is thought to be mediated by localized actin polymerization that pushes plasma membrane outward (Sechi and Wehland, 2000). Consistent with such a mechanism, wortmannin and LY294002 inhibited phagocytosis, but did not inhibit the increase in F-actin content that followed addition of anti-E IgG (Figure 4B). This indicated that pseudopod extension for Fcγ receptor-mediated phagocytosis occurs by a PI 3-kinase-independent stimulation of actin polymerization, presumably localized beneath the phagosomal membrane.

We were surprised to find that actin polymerization in response to M-CSF was inhibited by wortmannin and LY294002. M-CSF stimulates ruffling and macropinocytosis in macrophages (Racoosin and Swanson, 1989). The increase in cellular F-actin in response to M-CSF is consistent with an association between actin polymerization and ruffling, a cellular response that is analogous to pseudopod extension. However, although wortmannin does not inhibit cell surface ruffling (Araki *et al.*, 1996), it did inhibit the M-CSF–induced increases in macrophage F-actin (Figure 4C). This indicates that macrophage ruffling in wortmannin occurs without a net increase in F-actin. Increased rates of actin polymerization could still drive ruffle extension in wortmannin-treated cells, but they would have to be balanced by equal increases in the rates of depolymerization. The role of PI 3-kinase in actin polymerization during ruffling and pseudopod extension merits further study.

Although a number of myosins have been associated with phagosomes (Stendahl *et al.*, 1980; Allen and Aderem, 1995; Swanson *et al.*, 1999), their contributions to phagocytosis remain undefined. We previously immunolocalized three unconventional myosins (IC, V, IXb) and nonmuscle myosin II in macrophages during Fcγ receptor-mediated phagocytosis (Swanson *et al.*, 1999). In those studies, no class of myosin labeled all phagosomes. Rather, it appeared that the various myosin isoforms were recruited to phagosomes at different times, and left the phagosome with different kinetics. Synchronized phagocytosis and immunofluorescence demonstrated that the various myosins associated with phagosomes asynchronously, arriving and departing with different kinetics. The first peak of association of myosins II and IXb with phagosomes occurred 20 s after addition of IgG, which correlated with the peak of F-actin staining of phagocytic cups. This timing is consistent with a role for myosin II or IXb in regulating or modulating pseudopod extension. In this context, it is noteworthy that myosin IXb has Rho-GAP activity (Post *et al.*, 1998). Thus, myosin IXb may help shape the phagosome by

locally modulating the activities of actin regulatory proteins. Myosin IC localization peaked initially at 30 s, consistent with its postulated role in mediating phagosome closure (Swanson *et al.*, 1999). Myosin V association increased continuously during 3 min, indicating that it may have more to do with the dynamics of fully internalized phagosomes than with the mechanism of phagocytosis.

All of the myosins showed a gradual increase in their association with phagosomes over time. We presently do not know the significance of these later associations. Immunolocalization in wortmannin-treated macrophages showed little or no association of any myosin with phagocytic cups at any time point. This indicates that the changing percentages of immunolocalization in uninhibited cells, even at late time points, reflect phagocytosis-associated dynamics.

One additional class of unconventional myosin whose dynamics pertain herein is myosin X, which contains a pleckstrin homology domain that recognizes PI 3,4,5-P_3 specifically (Berg *et al.*, 2000), and which associates with phagosomes during phagocytosis (Cox *et al.*, 2000). We expect that association of myosin X with phagosomes would resemble that of myosin 1C and would be inhibited by wortmannin treatment.

The Rho family of small GTPases, which include RhoA, Rac1, and Cdc42 among others, are established mediators of actin reorganization in a wide range of cellular responses to stimuli (Hall, 1998). Rac1 and Cdc42 have been implicated in Fcγ receptor-mediated phagocytosis; evidence of a role for Rho is equivocal (Chimini and Chavrier, 2000). A number of cytoskeletal regulatory proteins modulate, or are modulated by, Rho-family GTPases, and these may control essential elements of Fcγ receptor-mediated phagocytosis. GTP-Rac and GTP-Cdc42 activate PAK1 (Manser *et al.*, 1994), which has been shown to be associated with phagosomes in neutrophils (Dharmawardhane *et al.*, 1999), and to contribute to macropinocytosis (Dharmawardhane *et al.*, 2000). In fibroblasts and neutrophils, PAK1 association with the actin cytoskeleton, and with phagosomes in particular, is inhibited by cytochalasin D and by wortmannin (Dharmawardhane *et al.*, 1997, 1999). In the present study, PAK1 localized to forming phagosomes in macrophages then disappeared from them before phagocytosis was complete. Inhibition of PI 3-kinase with wortmannin did not inhibit association of PAK1 with phagosomes, but instead prevented PAK1 loss from phagocytic cups. The differences between these results and the findings of Dharmawardhane *et al.* (2000) indicate different effects of PI 3-kinase in neutrophils and macrophages on PAK1 localization to phagosomes. If the PAK1 that persists in phagocytic cups of wortmannin-treated cells remains active then it may continually inhibit the activity of myosin light chain kinase (Sanders *et al.*, 1999), consequently reducing contractile activities necessary for phagosome closure.

Ezrin regulates associations of the actin cytoskeleton with a variety of membrane proteins. Its association with type 1 membrane proteins and with actin is regulated by phosphorylation and by association with PI 4,5-P_2 (Tsukita and Yonemura, 1999; Bretscher *et al.*, 2000). Ezrin association with latex bead-containing phagosomes in macrophages mediates associations of those phagosomes with F-actin (Defacque *et al.*, 2000). In the present study, ezrin association with phagosomes appeared to remain elevated after initiation of phagocytosis, consistent with a continued role for ezrin in phagosome function. The effects of wortmannin on ezrin association with phagosomes were difficult to interpret; it appears that there was a partial inhibition of ezrin association with phagosomes.

PI 3-kinase is activated by many tyrosine kinase-mobilizing receptors that mediate F-actin assembly (Cantrell, 2001). In most cases, PI 3-kinase activity is essential for activation of Rac after ligation of tyrosine kinase receptors. The macrophage's ability to polymerize actin and to extend pseudopodia in the presence of PI 3-kinase inhibitors indicates that some Rho family activities occur independent of PI 3-kinase. We suggest that Fcγ receptor ligation activates Cdc42 in a PI 3-kinase-independent manner, allowing some actin polymerization and pseudopod extension, and activates Rac in a PI 3-kinase-dependent manner. This model would predict that dominant negative Cdc42 should inhibit pseudopod extension, but dominant negative Rac should not, and that wortmannin should inhibit activation of Rac but not Cdc42. A similar model, and data consistent with this model, were presented by Massol *et al.* (1998), in a study of Fcε receptor-mediated phagocytosis in RBL-2H3 cells. Activation of Cdc42 would allow activation of PAK1, which in turn would inhibit myosin light chain kinase and the contractility necessary for phagosome closure. A delayed increase in PI 3-kinase activity would lead to activation of Rac1 and deactivation or delocalization of PAK1, releasing the inhibition of myosin activities and permitting phagosome closure.

Although these methods allow biochemical analyses of the molecular events during phagocytosis, it should be noted that they might not be ideal for study of FcR signaling. Because this method tethers erythrocytes via CR3, the FcR-mediated phagocytosis that follows could entail signaling by both FcR and CR3 (Jones *et al.*, 1998). With this in mind, however, a number of proteins implicated in phagocytosis can be analyzed for the timing of their association with phagosomes and the sensitivity of those associations to inhibitors of PI 3-kinase. This could provide a temporal and spatial ordering of the signal transduction elements that are coordinated to form a phagosome. Such quantitative studies should complement microscopic methods that follow the behavior of fluorescent probes in forming phagosomes, which give more precise indications of timing, but that are constrained by limited sample sizes.

ACKNOWLEDGMENTS

REFERENCES

Aderem, A., and Underhill, D.M. (1999). Mechanisms of phagocytosis in macrophages. Annu. Rev. Immunol. *17*, 593–623.

Allen, L.-A.H., and Aderem, A. (1995). A role for MARCKS, the α isozyme of protein kinase C and myosin I in zymosan phagocytosis by macrophages. J. Exp. Med. *182*, 829–840.

Araki, N., Johnson, M.T., and Swanson, J.A. (1996). A role for phosphoinositide 3-kinase in the completion of macropinocytosis and phagocytosis in macrophages. J. Cell Biol. *135*, 1249–1260.

Bajno, L., Peng, X.-R., Schreiber, A.D., Moore, H.-P., Trimble, W.S., and Grinstein, S. (2000). Focal exocytosis of VAMP3-containing vesicles at sites of phagosome formation. J. Cell Biol. *149*, 697–705.

Berg, J.S., Derfler, B.H., Pennisi, C.M., Corey, D.P., and Cheney, R.E. (2000). Myosin-X, a novel myosin with pleckstrin homology domains, associates with regions of dynamic actin. J. Cell Sci. *113*, 3439–3451.

Botelho, R.J., Teruel, M., Dierckman, R., Anderson, R., Wells, A., York, J.D., Meyer, T., and Grinstein, S. (2000). Localized biphasic changes in phosphatidylinositol-4,5-bisphosphate at sites of phagocytosis. J. Cell Biol. *151*, 1353–1367.

Bretscher, A., Chambers, D., Nguyen, R., and Reczek, D. (2000). ERM-Merlin and EBP50 protein families in plasma membrane organization and function. Annu. Rev. Cell Dev. Biol. *16*, 113–143.

Cano, M., Cassimeris, L., Joyce, M., and Zigmond, S. (1991). Characterization of TRITC-phalloidin binding to cellular F-actin. Cell Motil. Cytoskeleton *21*, 147–158.

Cantrell, D.A. (2001). Phosphoinositide 3-kinase signaling pathways. J. Cell Sci. *114*, 1439–1445.

Chimini, G., and Chavrier, P. (2000). Function of Rho family proteins in actin dynamics during phagocytosis and engulfment. Nat. Cell Biol. *2*, E191–E196.

Cox, D., Berg, J.S., Dale, B.M., Cheney, R.E., and Greenberg, S. (2000). A role for myosin-X in phagocytosis and pseudopod extension. Mol. Biol. Cell *11*, 375a.

Cox, D., Tseng, C.-C., Bjekic, G., and Greenberg, S. (1999). A requirement for phosphatidylinositol 3-kinase in pseudopod extension. J. Biol. Chem. *274*, 1240–1247.

Crowley, M.T., Costello, P.S., Fitzer-Attas, C.J., Turner, M., Meng, F., Lowell, C., Tybulewicz, V.L.J., and DeFranco, A.L. (1997). A critical role for Syk in signal transduction and phagocytosis mediated by Fcγ receptors on macrophages. J. Exp. Med. *186*, 1027–1039.

Defacque, H., et al. (2000). Involvement of ezrin/moesin in de novo actin assembly on phagosomal membranes. EMBO J. *19*, 199–212.

Dharmawardhane, S., Brownson, D., Lennartz, M., and Bokoch, G.M. (1999). Localization of p21-activated kinase 1 (PAK1) to pseudopodia, membrane ruffles, and phagocytic cups in activated human neutrophils. J. Leukocyt. Biol. *66*, 521–527.

Dharmawardhane, S., Sanders, L.C., Martin, S.S., Daniels, R.H., and Bokoch, G.M. (1997). Localization of p21-activated kinase-1 (PAK-1) to pinocytic vesicles and cortical actin structures in stimulated cells. J. Cell Biol. *138*, 1265–1278.

Dharmawardhane, S., Schurmann, A., Sells, M.A., Chernoff, J., Schmid, S.L., and Bokoch, G.M. (2000). Regulation of macropinocytosis by p21-activated kinase-1. Mol. Biol. Cell *11*, 3341–3352.

Edwards, D.C., Sanders, L.C., Bokoch, G.M., and Gill, G.M. (1999). Activation of LIM-kinase by Pak1 couples Rac/Cdc42 GTPase signaling to actin cytoskeletal dynamics. Nat. Cell Biol. *1*, 253–259.

Espreafico, E., Cheney, R., Matteoli, M., Nascimento, A., DeCamilli, P., Larson, R., and Mooseker, M.S. (1992). Primary structure and cellular localization of chicken brain p190 (Myosin-V), an unconventional myosin heavy chain with associated calmodulin light chains. J. Cell Biol. *119*, 1541–1558.

Greenberg, S., El Khoury, J., DiVirgilio, F., Kaplan, E.M., and Silverstein, S.C. (1991). Ca^{++}-independent F-actin assembly and disassembly during Fc receptor-mediated phagocytosis in macrophages. J. Cell Biol. *113*, 757–767.

Hall, A. (1998). Rho GTPases and the actin cytoskeleton. Science *279*, 509–514.

Howard, T.H., and Oresajo, C.O. (1985). The kinetics of chemotactic peptide-induced change in F-actin content, F-actin distribution, and the shape of neutrophils. J. Cell Biol. *101*, 1078–1085.

Jones, S.L., Knaus, U.G., Bokoch, G.M., and Brown, E.J. (1998). Two signaling mechanisms for activation of $\alpha_M\beta_2$ avidity in polymorphonuclear neutrophils. J. Biol. Chem. *273*, 10556–10566.

Kimura, K., et al. (1996). Regulation of myosin phosphatase by Rho and Rho-associated kinase (Rho-kinase). Science *273*, 245–248.

Knapp, P.E., and Swanson, J.A. (1990). Plasticity of the tubular lysosomal compartment in macrophages. J. Cell Sci. *95*, 433–439.

Lowry, M.B., Duchemin, A.M., Robinson, J.M., and Anderson, C.L. (1998). Functional separation of pseudopod extension and particle internalization during Fcγ receptor-mediated phagocytosis. J. Exp. Med. *187*, 161–176.

Manser, E., Leung, T., Salihuddin, H., Zhao, Z.S., and Lim, L. (1994). A brain serine/threonine protein kinase activated by Cdc42 and Rac1. Nature *367*, 40–46.

Massol, P., Montcourrier, P., Guillemot, J.-C., and Chavrier, P. (1998). Fc receptor-mediated phagocytosis requires CDC42 and Rac1. EMBO J. *17*, 6219–6229.

May, R.C., and Machesky, L.M. (2001). Phagocytosis and the actin cytoskeleton. J. Cell Sci. *114*, 1061–1077.

Ostap, E.M., and Pollard, T.D. (1996). Overlapping functions of myosin-I isoforms? J. Cell Biol. *133*, 221–224.

Post, P.L., Bokoch, G.M., and Mooseker, M.S. (1998). Human myosin-IXb is a mechanochemically active motor and a GAP for rho. J. Cell Sci. *111*, 941–950.

Racoosin, E.L., and Swanson, J.A. (1989). Macrophage colony stimulating factor (rM-CSF) stimulates pinocytosis in bone marrow-derived macrophages. J. Exp. Med. *170*, 1635–1648.

Sanders, L.C., Matsumura, F., Bokoch, G.M., and deLanerolle, P. (1999). Inhibition of myosin light chain kinase by p21-activated kinase. Science *283*, 2083–2085.

Sechi, A.S., and Wehland, J. (2000). The actin cytoskeleton and plasma membrane connection: PtdIns(4,5)P2 influences cytoskeletal protein activity at the plasma membrane. J. Cell Sci. *113*, 3685–3695.

Skowron, J.F., Bement, W.M., and Mooseker, M.S. (1998). Human brush border myosin-I and myosin-Ic expression in human intestine and Caco-2$_{BBe}$ cells. Cell Motil. Cytoskeleton *41*, 308–324.

Stendahl, O.I., Hartwig, J.H., Brotschi, E.A., and Stossel, T.P. (1980). Distribution of actin-binding protein and myosin in macrophages during spreading and phagocytosis. J. Cell Biol. *84*, 215–224.

Swanson, J.A. (1989). Phorbol esters stimulate macropinocytosis and solute flow through macrophages. J. Cell Sci. *94*, 135–142.

Swanson, J.A., and Baer, S.C. (1995). Phagocytosis by zippers and triggers. Trends Cell Biol. *5*, 89–93.

Swanson, J.A., Johnson, M.T., Beningo, K., Post, P., Mooseker, M., and Araki, N. (1999). A contractile activity that closes phagosomes in macrophages. J. Cell Sci. *112*, 307–316.

Tsukita, S., and Yonemura, S. (1999). Cortical actin organization: lessons from ERM (ezrin/radixin/moesin) proteins. J. Biol. Chem. *274*, 34507–34510.

Wirth, J.A., Jensen, K.A., Post, P.L., Bement, W.M., and Mooseker, M.S. (1996). Human myosin-IXb, an unconventional myosin with a chimerin-like rho/rac GTPase-activating protein domain in its tail. J. Cell Sci. *109*, 653–661.

Wright, S.D., and Griffin, F.M. (1985). Activation of phagocytic cells' C3 receptors for phagocytosis. J. Leukoc. Biol. *38*, 327–339.

Wright, S.D., and Silverstein, S.C. (1982). Tumor-promoting phorbol esters stimulate C3b and C3b' receptor-mediated phagocytosis in cultured human monocytes. J. Exp. Med. *156*, 1149–1164.